ELSEVIER

Journal of Fluids and Structures 22 (2006) 773–782

JOURNAL OF FLUIDS AND STRUCTURES

www.elsevier.com/locate/jfs

On vortex-induced vibrations of cylinders describing X–Y trajectories

A. Laneville*

Génie mécanique, Université de Sherbrooke, 2500 boul Université, Sherbrooke, Province de Québec, Canada J1K 2R1

Received 29 September 2005; accepted 9 April 2006
Available online 27 July 2006

Abstract

This paper examines the 2S and 2P wake flow modes and their respective domain under configurations differing from that of free oscillations in the cross-flow direction only. A proposed dimensionless variable, α, defining a velocity plane of vibration is shown to link results obtained under X–Y motion to observations made with mechanically constrained oscillations. This variable, α, attempts to evaluate how far the conditions of motion are from that of a pure Y motion and associates the corresponding modes of vortex shedding: this variable corresponds to $\arctan[(\mathrm{d}X/\mathrm{d}t)/(\mathrm{d}Y/\mathrm{d}t)]$. The 2P mode is observed to cease to occur as the transverse vibration plane is inclined at angles $\alpha > 30^\circ$ with respect to the cross-flow direction. Although the onset of vortex-induced vibrations is observed to remain identical in the range $0 \leqslant \alpha \leqslant 45^\circ$, the synchronization range is reduced with increasing α. The critical curve, detected from the experimental occurrence of bifurcations, is gradually shifted as α is increased.

Keywords: Vortex-induced vibrations; Vortex shedding modes; X–Y motion; Critical curve

1. Introduction

In the case of airflows impinging on a cylindrical structure free to vibrate, three modes of vortex shedding have been observed: the Kármán mode if the structure is at rest, and the 2S and 2P modes if the structure oscillates in resonance in the transverse direction. The 2S mode is characterized by the shedding of two single vortices per cycle of oscillation, and the 2P mode by the shedding of two pairs of vortices. Williamson and Roshko (1988) used their flow visualization results to draw a map (A/D, U) of these modes and a particular boundary separating the 2S from the 2P modes: this is the "critical curve" which was later measured by Brika and Laneville (1993).

In order to examine the limiting conditions of existence of the 2S and 2P modes and the consecutive modifications to the "critical curve", one has to revisit the vortex formation process in the case of the well investigated Kármán mode. Zdravkovich (1997) gives an in-depth discussion of the process of the vortex formation: in the particular range of Reynolds numbers typical for overhead lines (4000–15 000), the boundary layer from the point of stagnation to the point of separation remains laminar. Ballengee and Chen (1971) have measured the location of the separation point: its angle from the stagnation point varies almost linearly with Reynolds number, from 91° at $\mathrm{Re} = 10^4$ to 83° at $\mathrm{Re} = 3.9 \times 10^4$. The shear layer proceeding from the point of separation undergoes transition and rolls on itself to form

*Tel.: +1 819 821 8000x62153; fax: +1 819 821 7163.
E-mail address: andre.laneville@USherbrooke.ca.

0889-9746/$ - see front matter
doi:10.1016/j.jfluidstructs.2006.04.018

a vortex that is shed downstream in the wake. The state of the boundary layer upstream of separation will logically influence the amount of vorticity contained in the released vortices as well as their configuration. In support, small velocity perturbations contained in the oncoming flow such as small-scale turbulence, were shown to enter the boundary layer via the stagnation point and to modify the properties of the shear layer (Laneville et al., 1975) in the case of rectangular prisms where the location of the separation point is fixed.

As the cylindrical structure is set in motion, the stagnation and separation points are also displaced and the shear generated in the boundary layer should be modified from that of the stationary structure. This implies that the vorticity at the separation point, and consequently the mode of vortex shedding, should be influenced by both the oncoming flow velocity and that of the moving surface. Following this line of reasoning, we anticipate some dislocation of the wake in the case of X–Y motion of the structure. The available experimental results that will be discussed later in more detail, lead to different conclusions: in some cases, the additional freedom for the structure to oscillate in the X direction or in-line with the flow hardly affects the vortex shedding modes observed in Y motion only; in other cases, it can inhibit one of the vortex shedding modes.

This paper focuses on the 2S and 2P modes of vortex shedding and the effect on their existence of perturbing the Y motion by allowing an X motion. This effect will be analogous to that of a velocity plane of vibration making an angle α with the cross-flow vibrations. A dimensionless variable will be proposed to link this velocity plane of vibration to that of oscillations mechanically constrained at different angles with the flow. The critical curve and the amplitudes of vibration for these different planes will be revisited in order to identify the limits of existence of the 2S and 2P modes of vibration. This dimensionless variable will be applied to available data and will be used to reconcile some differing results.

2. Background

In the case of a given cylindrical structure (D, L, m_L) vibrating (ω_v, ζ) freely and steadily in an airflow (ρ, v, V), the main dimensionless variables controlling the phenomenon are the reduced velocity ($U = V/D\omega_v$), the Scruton number ($2m_L\zeta/(\rho D^2)$), the Strouhal number ($f_{SVS}D/V$), and the Reynolds number (VD/v), while the dependent variable is the reduced amplitude (A/D). The Strouhal frequency, f_{SVS}, corresponds to the vortex shedding frequency in the cases of the structure at rest. In contrast to the cases of liquid flows, the mass parameter [$m^* = 4m_L/(\pi\rho D^2)$] does not play a significant role and the vibrating frequency corresponds practically to the natural frequency of the structure. The reduced velocity, or its equivalent, and the reduced amplitude are the two variables used to describe the critical curve in Williamson and Roshko (1988) since it was obtained under forced oscillations in a towing water channel.

3. The critical curve

In the experiment by Williamson and Roshko (1988), the flow velocity relative to the vertical cylinder was the combination of a constant towing velocity and a forced transverse oscillation in order to generate a sinusoidal trajectory. For a given cylinder, there were three independent or controlling variables in this experiment: the towing velocity, and the frequency and amplitude of the forced oscillations. The water adopts the role of dissipating the power imposed on the cylinder. The methodology can be summarized thus: once the water surface of the towing tank was covered with aluminium particles, the vertical cylinder and its carriage were forced into motion and photographs of the patterns in the wake were taken. Analyses of the photographed patterns have led to the definition of three principal modes of vortex shedding in the synchronization region: the 2S, 2P and P + S modes: Fig. 1 shows the original map of the vortex shedding modes for this region with the critical curve identified as the boundary separating the 2S from the 2P modes. The authors adopted the nomenclature λ/D, an equivalent to $2\pi U \times$ Strouhal number, for the abscissa.

The critical curve deduced by Williamson and Roshko (1988) was detected by Brika and Laneville (1993) using a different avenue: the occurrence of bifurcations in the unsteady response of the flexible cylinder and their coupling with a jump in the phase angle was identified as the crossing of the critical curve. Recordings of flow visualization taken prior and posterior to the bifurcation confirmed the presence of the two different modes of vortex shedding. Bifurcations were previously reported by several authors [Ferguson (1965), Diana and Falco (1971), among others]. Fig. 2 shows the recording of such a bifurcation for $U = 0.87$ (in this case $V/f_C D = 2\pi U$).

These bifurcations were detected in the range of velocities $0.84 < U < 0.87$ and their amplitude, along with the measured steady amplitudes, were superimposed on the map proposed by Williamson and Roshko (1988) in Fig. 3. The agreement between the critical curve and the measured bifurcations is remarkable. Moreover, the plateau $A/D \approx 0.4$ of the lower branch of the hysteresis loop is observed to begin with the critical curve ($U = 0.86$) and to end more or less with the boundary of the region for which synchronization requires a very large number of cycles if ever it can be achieved.

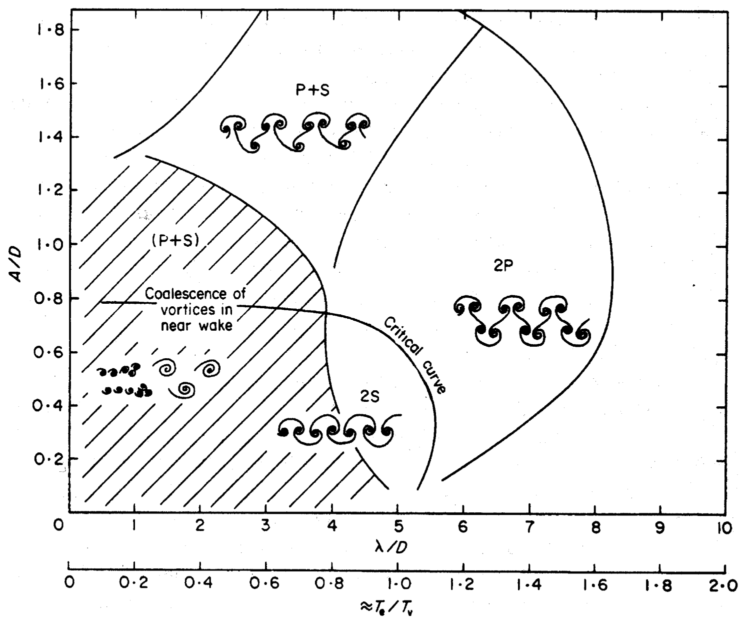

Fig. 1. Map of vortex shedding modes after Williamson and Roshko (1988).

4. Cases of X–Y motions and planes of vibration at $\alpha \neq 0$

The critical curve has been well established and validated in the case of vibrations in a transverse plane perpendicular ($\alpha = 0$) to the oncoming flow; the effect of an X–Y motion or of tilting the transverse plane at an angle α will be discussed once a dimensionless variable is chosen.

Harmonic X–Y motions can be described by the two components of the amplitude, A_x and A_y, and that of the vibrating frequencies, ω_x and ω_y. Three dimensionless variables can be obtained by simple inspection: the ratio of the amplitudes A_x/A_y, the ratio of the vibrating frequencies ω_x/ω_y, and finally the ratio of the velocities $\omega_x A_x/(\omega_y A_y)$. A more general definition would simply be the ratio of the average motion speeds $(\mathrm{d}X/\mathrm{d}t)/(\mathrm{d}Y/\mathrm{d}t)$ over one cycle. The average speed, $\mathrm{d}X/\mathrm{d}t$, corresponds to the length of the described X trajectory $(4A_x)$ over its period $(2\pi/\omega_x)$. The latter dimensionless ratio, in addition to combining the first two variables, can be expected intuitively to play a more important role since the shear in the boundary layer before the vortex formation is velocity dependent. If α is the angle made by this velocity ratio as measured from the vertical (Y) direction, then α defines a plane of vibration that corresponds to the physical plane of the tests reported by Brika and Laneville (1995). One may write simply

$$\tan\alpha = (\mathrm{d}X/\mathrm{d}t)/(\mathrm{d}Y/\mathrm{d}t) = \omega_x A_x/(\omega_y A_y).$$

If the X and Y motions are made interdependent, as in the case of the X motion solidly coupled to the Y motion, then only one frequency describes the two motions ($\omega_x = k\omega_y$) and

$$\tan\alpha = (\mathrm{d}X/\mathrm{d}t)/(\mathrm{d}Y/\mathrm{d}t) = kA_x/A_y.$$

For structures with a square or a circular cross-section, the value of k is 1. This variable, α, attempts to evaluate how far the conditions of motion are from that of pure Y motion and associates the corresponding modes of vortex shedding in the next paragraphs and Fig. 6.

One of the earlier studies of forced vibrations of a circular cylinder in a non-orthogonal plane has been made by Öngören and Rockwell (1988a,b). They observed the presence of different vortex patterns of the symmetrical and anti-symmetrical types in the wake of the cylinder and, as α, the vibration plane angle with respect to the cross-flow direction, is increased, they noted that a competition between the vortex shedding modes grows stronger.

In a recent review, Sarpkaya (2004) reports on the data he obtained previously (Sarpkaya, 1995) in a water flow with a cylinder free to vibrate at the same natural frequency in two orthogonal directions: "the variation of A/D with" the dimensionless velocity "St $\times$ $V/f_C D$" "yields about 20% larger amplitude over a 20% range of the velocity for a Reynolds number of about 35 000".

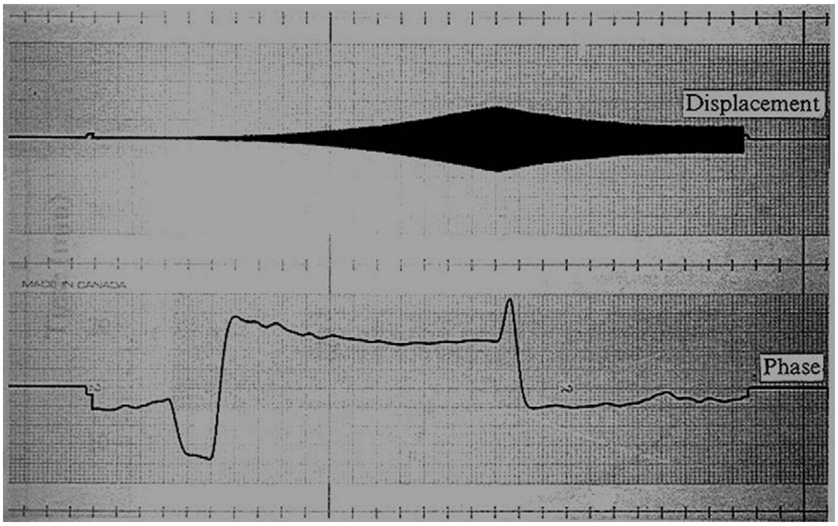

Fig. 2. Bifurcation in the response coupled with jump in the phase signals after Brika and Laneville (1993) for $U = 0.87$.

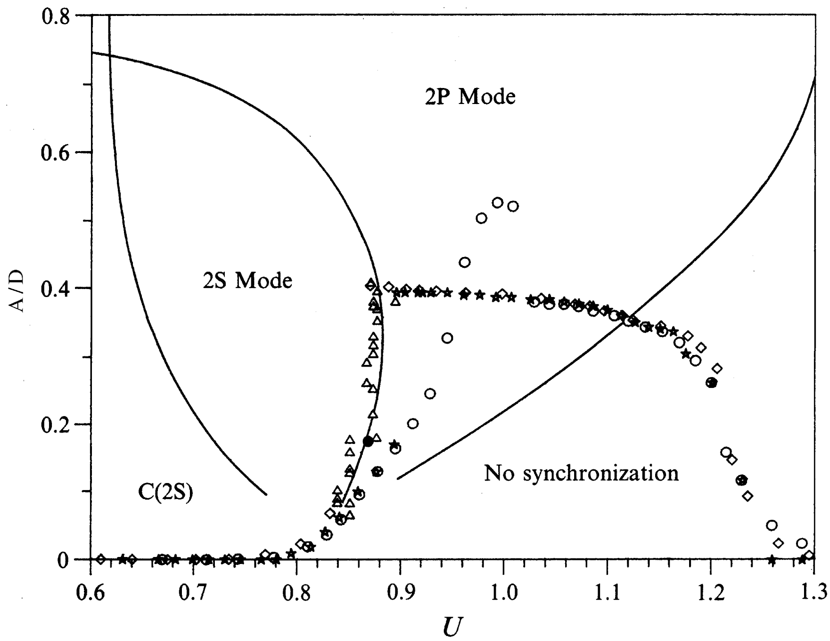

Fig. 3. Comparison of the experimental results: filled circle, bifurcation amplitude (Ferguson (1965)); open triangles, bifurcation amplitudes (Brika and Laneville (1993)); line, Williamson and Roshko (1988); other symbols, steady state amplitudes (Brika and Laneville (1993)).

According to Williamson and Govardhan (2004), two recent studies using "arrangements that ensure" "the same mass ratio and the same natural frequency" in both X and Y directions "demonstrate a set of response branches" and "that the freedom to oscillate in-line with the flow hardly affects the response branches, the forces, and the vortex wake modes". A link seems to be missing in order to reconcile these differing observations.

Brika and Laneville (1995) reports on an experimental study of the Aeolian vibrations (VIV in the case of aerial cables) using the identical set-up of Brika and Laneville (1993) but with the transverse plane of vibration mounted at different angles α with the cross-flow. In their tests, the frequencies of X and Y motions were interdependent and the Reynolds number ranged from 3700 to 12 000. Since this is the only set of data covering a large range of α to the author's knowledge, their results will be summarized. Fig. 4 shows their measurements and the principal observations follow in a point-wise format.

1. For all the angles α tested, synchronization occurs over a range of wind speed.
2. For all the angles α tested, synchronization onsets at $U = 0.79$, that is when the Strouhal frequency approaches the cylinder natural frequency, as opposed to $U \cos \alpha$. The reference velocity should be the oncoming flow velocity.

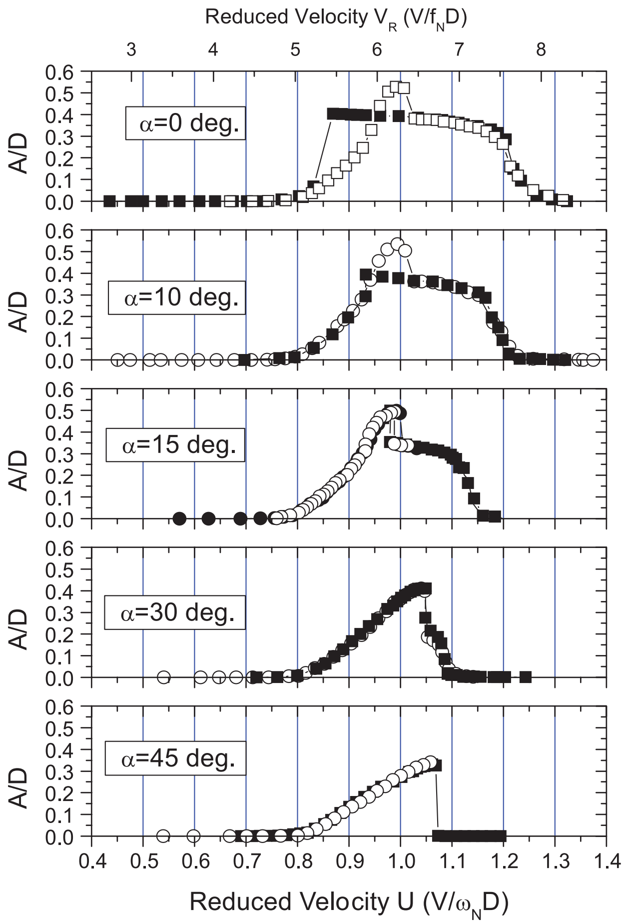

Fig. 4. Steady state amplitudes for different incident angles of the plane of vibration (α in deg.).

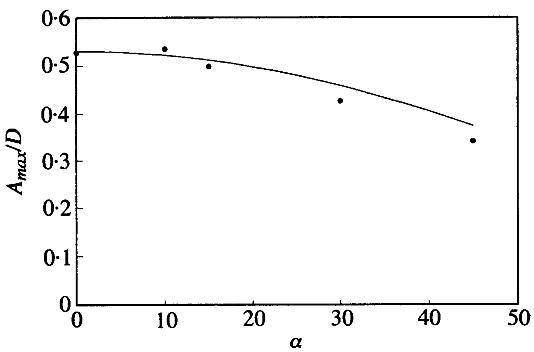

Fig. 5. Comparison between the maximum amplitude measured and $(A/D)_{\max|\alpha=0} \cos\alpha$ (Brika and Laneville, 1995).

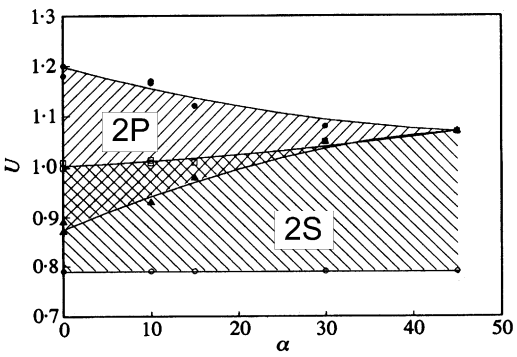

Fig. 6. Effect of α on the regions of lock-in: ◦, onset of lock-in; ●, end of synchronization; ▲, LCV; □, UCV (Brika and Laneville, 1995).

3. Synchronization ends at a flow velocity the value of which decreases as α is increased.
4. The maximum amplitude measured in each plane of vibration reduces as the value of α is increased; Fig. 5 shows that the measured values are in good agreement with the curve defined as $(A/D)_{\max|\alpha=0} \times \cos\alpha$.
5. Two branches of a hysteresis loop are present for planes of vibration with $\alpha \leqslant 30^\circ$. The hysteresis can be deduced to cease to exist for larger values of α as in the case of $\alpha = 45^\circ$.
6. Jumps between the two branches are present but the value of the velocity U is a function of α, again for $\alpha \leqslant 30^\circ$.
7. The lowest critical velocity, LCV, defined as the lowest velocity for the lower branch, increases continuously with α; this implies that the critical curve is shifting and that the domain of the 2P mode of vortex shedding is shrinking as the value of α is increased. For $\alpha > 30^\circ$, the 2P mode does not occur.
8. The upper critical velocity, UCV, defined as the highest velocity for the upper branch increases slowly with α. For $\alpha = 30^\circ$, the condition UCV $\approx$ LCV is almost met and the 2P mode becomes almost extinct.

These observations are regrouped in Fig. 6 in order to visualize their significance. The domain of the 2S mode (hatching with a negative slope and bordered by the onset velocity and UCV) expands with α, as opposed to the domain of the 2P mode (hatching with a positive slope and bordered by LCV and the end of synchronization) that is shrinking. For $\alpha = 30^\circ$, the 2P mode can be inferred to occur in a narrow range of velocities ($1.05 \leqslant U \leqslant 1.1$). Consequently, the double amplitude domain (cross hatching) becomes narrower as the transverse plane of vibration is tilted to larger incidence angles.

When the blades of the supporting system were inclined at $\alpha = 45^\circ$ with respect to the incoming flow, Brika and Laneville (1995) observed their flexible cylinder to vibrate in two different and stable planes, the first corresponding to the constraint by the blades ($\alpha = +45^\circ$) and the second almost perpendicular to the first ($\alpha = -45^\circ$). The cylinder was describing an elliptical trajectory in both planes.

The vibrations in the plane $\alpha = 45^\circ$ are midway between the orthogonal vibrations characterized by antisymmetrical modes of vortex-shedding and the in-line vibrations with symmetrical modes of vortex shedding. Öngören and Rockwell (1988b) observed a competition between these modes for non-orthogonal vibrations, and according to Fig. 30 of this reference, the maximum competition between symmetrical and antisymmetrical modes occurs at about $U = 1.10$, a velocity 3% higher than the end of synchronization velocity of the present Fig. 6.

The wake of the oscillating cylinder admittedly narrows as the angle of the vibration plane increases. The wake vortices should consequently be organized differently, allowing for a competition between different modes.

5. The critical curve for planes of vibration at $\alpha \neq 0$

To identify the location of the critical curve for the different values of α, the same methodology was adopted as the one for the cross-flow configuration. Impulsive tests were performed at fixed flow velocities. Some of the recorded traces of the cylinder displacement and of the phase angle are shown in Fig. 7.

It should be noted the amplitude does not stabilize directly on the upper (initial) branch, but there is a primary stability on the lower branch followed by a bifurcation and a final stability on the upper branch. As shown in Fig. 7, this bifurcation is accompanied by a sudden change of the phase angle, indicating an instantaneous variation of the

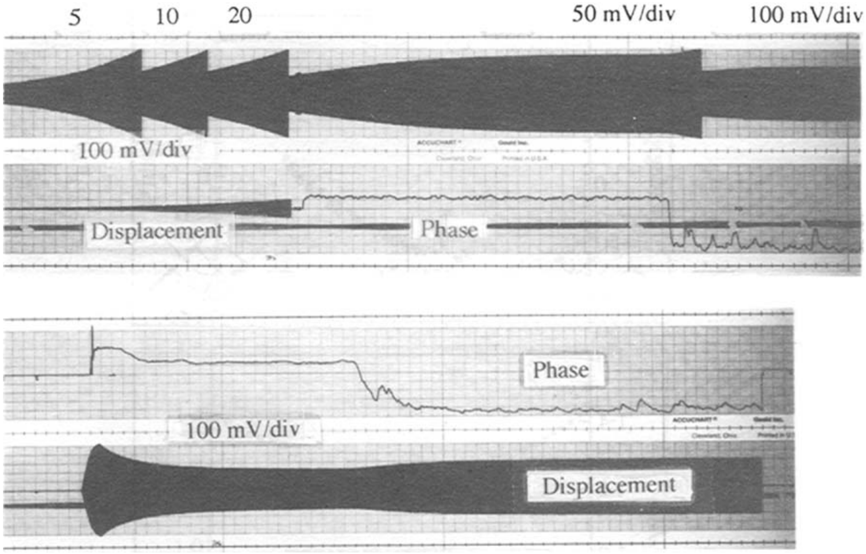

Fig. 7. Traces of displacement and phase angle (impulsive regimes, $\alpha = 15°$ and $U = 0.98$): top pair of traces, from rest; bottom pair, from high amplitude (Brika and Laneville, 1995).

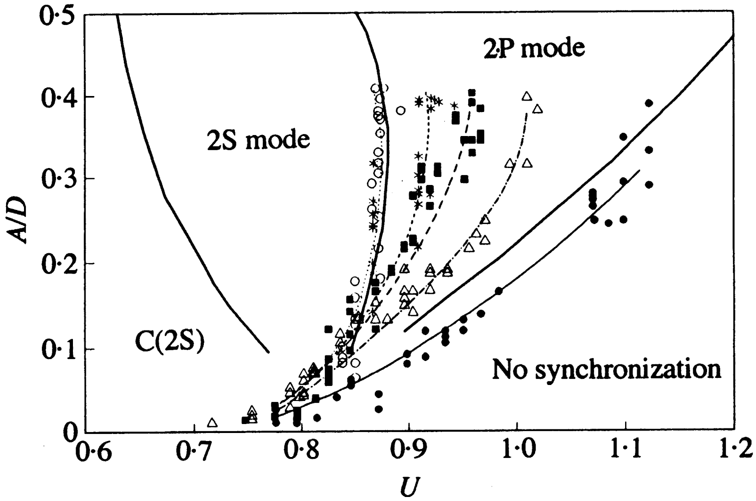

Fig. 8. Bifurcation amplitudes and the critical curve for different α in the map of the vortex shedding modes: ◦, $\alpha = 0$; *, $\alpha = 10°$; ■, $\alpha = 15°$; △, $\alpha = 30°$; ●, $\alpha = 45°$ (Brika and Laneville, 1995).

vortex configuration in the wake of the vibrating cylinder. This was observed either with a free excitation from rest (Fig. 7, top pair of traces) or with a pre-excitation at high amplitude (Fig. 7, bottom pair). Steady state conditions are assumed achieved when the vibration at given amplitude is maintained for more than 1000 cycles or more than 1 min.

By analysing the results of these impulsive regimes in the cases of $\alpha \neq 0$, new sets of bifurcation coordinates were determined and the location of the critical curve was defined for each α. Fig. 8 shows this compilation: the critical curve shifts towards higher values of U as α is increased. With this shift, the domain of the 2P mode of vortex shedding shrinks progressively with α: the measurements of the steady state amplitudes have already suggested this fact. For $\alpha = 45°$, the critical curve is now in the decoherence domain and the 2P mode is no longer present. For this particular α, the set of points corresponds to inflection points and not to bifurcation points. Their apparent scattering is attributed to the difficulty in determining the points of inflection.

6. Discussion

As the plane of vibration is inclined, a modification in the wake pattern is expected, the vortices being shed at each extreme of the cycle, approximately $2A\sin\alpha$ apart longitudinally but $2A\cos\alpha$ apart transversally. The wake can be inferred to be distorted as α is increased and the establishment of different spatial dispositions of the wake vortices is to be expected.

The wake transverse dimension at the peak amplitude of the 2S mode for $\alpha = 45°$ ($A/D = 0.34$, $U = 1.06$ and $A_x/A_y = 1$) is evaluated as $\sim 0.48D$ and is to be compared to $\sim 1.06D$ for $\alpha = 0°$ ($A/D = 0.53$, $U = 1.0$, $A_x/A_y = 0$). Similarly, one could evaluate the transverse dimension of the 2P mode as it almost ceases to exist at $\alpha = 30°$ ($A/D = 0.24$, $U = 1.07$, $A_x/A_y = 0.58$); this simple calculation yields $\sim 0.42D$, a value again to be compared to $\sim 0.6D$ for $\alpha = 0°$ ($A/D = 0.3$, $U = 1.18$). The 2S shedding mode has "survived" a 50% transverse narrowing of its wake while the 2P mode ceases to occur for a 30% transverse narrowing of its wake. This argumentation did not yet invoke the location of the point of separation and the local velocity. These observations would indicate that in the case of X–Y motions of a two-degree-of-freedom flexible cylinder with identical natural frequencies, the 2P mode would not occur if the amplitude of motion in the X direction reaches $\sim$60% of the one in the Y direction. It must be emphasised that the Reynolds number was varied from 3700 to 12 000 for these results.

The narrowing of the wake does not result solely from the geometrical motion of the cylinder as described by the ratio A_x/A_y; one could argue that a cylinder forced to oscillate at large amplitude but with a very slow frequency could shed almost Kármán vortices in its wake. As argued earlier, the shear in the boundary layer, the resultant vorticity at the point of separation and the configuration of the vortices in the wake should be influenced by two dimensionless velocity ratios, the reduced velocity U and $(\mathrm{d}X/\mathrm{d}t)/(\mathrm{d}Y/\mathrm{d}t)$. The latter turns out to be the amplitude ratio when both frequencies are identical; moreover, it corresponds to the value of $\tan\alpha$ in the experiments by Brika and Laneville (1995).

In order to discuss and compare the data obtained in different laboratories, the constraining effect made by the walls of the test-section has to be taken into account via a correction of the flow velocity. The solid blockage in the set up of Brika and Laneville (1995) is 2% and all the values of the velocity are nevertheless modified by a small correction. The same methodology (Pankhurst and Holder, 1962) will then be applied to all uncorrected data. This particular methodology has been selected principally for consistency: it is the correction technique used by Feng (1968) and whose work is widely referred to. This methodology might under-correct the velocity for blockage ratios larger than 10%.

Although the domains of existence of the different modes of vortex shedding are derived from tests using air as the flowing fluid, the proposed variable, α or $\arctan[(\mathrm{d}X/\mathrm{d}t)/(\mathrm{d}Y/\mathrm{d}t)]$, will be applied to the cases where a liquid is the flowing fluid.

Moe and Wu (1990) tested an aluminium cylinder mounted on a rig "functioning as a parallelogram" and permitting both X–Y and "approximately" Y motions in the Reynolds number range from 13 000 to 20 000. In the X direction, the minimum displacement could be reduced to $A_x/A_y = 0.035$ by preventing a joint from rotating in order to achieve "approximately" Y motions (interdependent motions); by allowing rotation at this joint, the degree of freedom in the X direction was gained and the cylinder could describe different motions (figure-of-eight among others). The vertical natural frequency in the still fluid, f_{nY}, is reported as 1.06 Hz and the ratio of the horizontal to the vertical natural frequencies as 2.18 (measured with an internal bi-directional balance in the still fluid). In the cases of Y and X–Y self-excitations, on one hand, the fundamental vibrating frequency in the Y direction was measured identical to f_{nY} using a displacement transducer; on the other hand, the FFT analysis of the signal from the internal balance contained a peak at f_{nY} for both motions and an additional peak at the second harmonic (3.18 Hz) in the cases of X–Y motions. The values of A_x and ω_x are not reported. For the only Y motion with data required to calculate α, the equivalent plane of vibration makes an angle α of 2°. Synchronization occurred in the reported range $4.9 \leqslant 2\pi U \leqslant 7.5$. Taking into account the solid blockage (7.1%), this range corresponds to $0.8 \leqslant U \leqslant 1.22$. Both ends of this range, the onset and the end of synchronization, agree with that of Fig. 6 of the present paper. In addition, an important reduction of A/D (from $\sim$0.7 to $\sim$0.35) occurs at $U = 0.95$ [$2\pi U = 5.8$, Fig. 5 of Moe and Wu (1990)]; the coordinates of this point are close to that of the UCV line indicating, in the case of an airflow, a change of vortex shedding modes from the 2S to the 2P. No flow visualization results are reported unfortunately.

Jeon and Gharib (2001) have tested circular cylinders undergoing X–Y forced motions with constant A_x/A_y $(= 0.2)$ and A/D $(= 0.5)$, but a frequency ratio of 2. Two tests are reported, the first for a velocity $U = 0.66$, and the second for $U = 0.955$. Once corrected for blockage (5%), the values of the velocity are respectively 0.67 and 0.97. In the original map of Williamson and Roshko (1988) obtained for pure Y motion, these conditions would fall in the domain of the 2S mode for the first test, and in that of the 2P mode for the second. In both tests, they detected only the 2S mode of vortex shedding. The variables U and A_y/D can then be concluded insufficient to describe entirely the phenomenon. The two test conditions in the experiment of Jeon and Gharib (2001) are ($U = 0.67$, $\alpha = 21.7°$) and ($U = 0.97$, $\alpha = 21.7°$);

referring to Fig. 6, none of these conditions has its coordinates in the domain of existence of the 2P mode. The second point lies in the 2S domain of the synchronization region while the first one remains outside the synchronization. The tests were done in the Reynolds number range from 800 to 1500.

Using a pendulum set-up that allows a cylinder to oscillate freely in the X–Y directions ($\omega_x/\omega_y = 1$, and $5 < m^* < 25$), Jauvtis and Williamson (2003) found both the 2S and 2P modes of vortex shedding in the synchronization region. Their tests were performed in the range $1000 <$ Reynolds number < 6000. Observing the agreement between the data obtained in pure Y and X–Y motions, they conclude to "the validity, for bodies in two degrees of freedom, of employing the existing comprehensive results for bodies restrained to vibrate only in the transverse Y direction, even down to low mass ratios of $m^* = 5$". One should notice that this conclusion results from tests with $\omega_x/\omega_y = 1$. For lower mass ratios, Williamson and Jauvtis (2004) observed the additional T mode of vortex shedding. Since this paper is concerned with airflows, the T mode of vortex shedding is not expected. Fig. 1 of Jauvtis and Williamson (2003) indicates amplitudes $A_x/D \sim 0.03$ and $A_y/D \sim 0.6$ for the lower branch; these conditions are equivalent to a plane of vibration making an angle α of 3 degrees. Since the models produced a solid blockage of 10% and 13.3%, correction methods for this level of blockage have a tendency to under-correct the velocity. Adopting nevertheless the same methodology, the data of Jauvtis and Williamson (2003) would indicate that the 2P mode extends from $U = 0.86$ to 1.47. According to Fig. 6, the value of the lower critical velocity in airflow for this α is ~ 0.89 while the end of synchronization is ~ 1.18. Because the angle of the plane of vibration is very close to 0, the modes of vortex shedding should closely resemble that observed in pure Y motion.

The apparently differing conclusions with respect to the 2P mode of vortex shedding made by Jeon and Gharib (2001) and by Jauvtis and Williamson (2003) can be reconciled using the second velocity ratio, $(\mathrm{d}X/\mathrm{d}t)/(\mathrm{d}Y/\mathrm{d}t)$ to determine the angle of the plane described by the vibration in combination with the map proposed by Brika and Laneville (1995).

Further tests and data are needed to validate this similitude criterion that allows us to determine the possible existence of the 2P and 2S modes of vortex shedding; although its application has been extended to cases where water rather than air was the flowing fluid, the effect of added mass and mass ratio might play a role as far as the end of synchronization is concerned. This similitude criterion nevertheless shows the relative importance of the kinematics of motion of the cylindrical structure in determining the mode of vortex shedding and the width of the wake.

7. Conclusion

The 2S and 2P modes of vortex shedding can be influenced by the X–Y motion of the cylindrical structure. The degree of this effect can be related to the time derivative of the motions, more precisely to their ratio $(\mathrm{d}X/\mathrm{d}t)/(\mathrm{d}Y/\mathrm{d}t)$. This ratio can be associated with a plane of oscillations defined by the two components of the structure velocity, $\mathrm{d}X/\mathrm{d}t$ and $\mathrm{d}Y/\mathrm{d}t$, and making an angle α with the Y direction. In the cases of interdependent X–Y motions, α corresponds to the ratio of the amplitudes kA_x/A_y. Using the concept of α, the existence of the 2S and 2P modes and the location of the critical curve can be determined from the observations made by Brika and Laneville (1995).

In the case of a flexible cylinder vibrating in a transverse plane to airflows but at an angle α to the cross-flow direction, the following observations can be deduced in the lock-in region.

(i) As compared with the case of oscillations in the cross-flow direction, only an increase of the angle α reduces the maximum amplitude of vibration and the range of the synchronisation region and of the double amplitude region, which disappears completely for $\alpha > 30^\circ$. For this condition, the 2P mode of vortex shedding was not observed, only the 2S mode.
(ii) Synchronization commences at the same velocity ($U = 0.79$). The value of U at the end of synchronisation decreases with increasing α.
(iii) The critical curve that defines the boundary between the 2S and 2P modes of vortex shedding was constructed for each angle α of the plane of vibration, using the bifurcations detected in the experimental results from the cylinder transient response. This curve was observed to shift towards higher velocities as α is increased.
(iv) The maximum amplitude of oscillation at each α can be estimated from the projection of the maximum amplitude of oscillation measured at $\alpha = 0^\circ$,
(v) The angle α can be related to the cases of the more conventional X–Y motions and can be used as a similitude criterion to establish the conditions of existence of the 2S and 2P modes of vortex shedding. This relationship is

$$\tan\alpha = (\mathrm{d}X/\mathrm{d}t)/(\mathrm{d}Y/\mathrm{d}t).$$

(vi) Using this criteria and the map proposed by Brika and Laneville (1995), the apparently differing conclusions with respect to the 2P mode of vortex shedding made by Jeon and Gharib (2001) and by Jauvtis and Williamson (2003) can be reconciled.

Acknowledgments

This research was supported by a grant from the Natural Sciences and Engineering Research Council of Canada. The author is grateful to Dr C. D. Williams for stimulating discussions and comments to improve the clarity of the manuscript.

References

Ballengee, D.W., Chen, C.F., 1971. Experimental determination of the separation point of flow around a circular cylinder. In: Dowdell, R.B. (Ed.), Flow; its Measurement and Control in Science and Industry, pp. 419–427.

Brika, D., Laneville, A., 1993. Vortex-induced vibrations of a long flexible circular cylinder. Journal of Fluid Mechanics 250, 481–508.

Brika, D., Laneville, A., 1995. An experimental investigation of the aeolian vibrations of a flexible circular cylinder at different incidences. Journal of Fluids and Structures 9, 371–391.

Diana, G., Falco, M., 1971. On the forces transmitted to a vibrating cylinder by a blowing fluid. Meccanica 6 (1), 9–22.

Feng, C.C., 1968. The measurement of vortex-induced effects in flow past a stationary and oscillating circular and D-section cylinders. Master's Thesis, U.B.C., Vancouver, Canada.

Ferguson, N., 1965. The measurement of wake and surface effects in the sub critical flow past a circular cylinder at rest and in vortex-excited oscillation. Master's Thesis, U.B.C., Vancouver, Canada.

Jauvtis, N., Williamson, C.H.K., 2003. Vortex-induced vibration of a cylinder with two degrees of freedom. Journal of Fluids and Structures 17, 1035–1042.

Jeon, D., Gharib, M.R., 2001. On circular cylinders undergoing two-degree-of-freedom forced motion. Journal of Fluids and Structures 15, 533–541.

Laneville, A., Gartshore, I.S., Parkinson, G.V., 1975. An explanation of some effects of turbulence on bluff bodies. In: Eaton, K.J. (Ed.), Proceedings Fourth International Conference on Wind Effects on Buildings and Structures. Cambridge University Press, pp. 333–341.

Moe, G., Wu, Z.-J., 1990. The lift force on a cylinder vibrating in a current. Journal of Offshore Mechanics and Artic Engineering 112, 297–303.

Öngören, A., Rockwell, D., 1988a. Flow structure from an oscillating cylinder. Part I: mechanisms of phase shift and recovery in near wake. Journal of Fluid Mechanics 191, 197–223.

Öngören, A., Rockwell, D., 1988b. Flow structure from an oscillating cylinder. Part 2: mode competition in the near wake. Journal of Fluid Mechanics 191, 225–245.

Pankhurst, R.C., Holder, D.W., 1962. Wind Tunnel Techniques. Pitman, London.

Sarpkaya, T., 1995. Hydrodynamic damping, flow-induced oscillations, and bi-harmonic response. Journal of Offshore Mechanics and Artic Engineering 117, 232–238.

Sarpkaya, T., 2004. A critical review of the intrinsic nature of vortex-induced vibrations. Journal of Fluids and Structures 19, 389–447.

Williamson, C.H.K., Govardhan, R., 2004. Vortex-induced vibrations. Annual Review of Fluid Mechanics 36, 413–455.

Williamson, C.H.K., Jauvtis, N., 2004. A high-amplitude 2T mode of vortex-induced vibration for a light body in X–Y motion. European Journal of Mechanics B/Fluids 23, 107–114.

Williamson, C.H.K., Roshko, A., 1988. Vortex formation in the wake of an oscillating cylinder. Journal of Fluids and Structures 2, 355–381.

Zdravkovich, M.M., 1997. Flow Around Circular Cylinders, vol. 1: Fundamentals. Oxford University Press, Oxford.